Jurnal Kejuruteraan 32(4) 2020: 629-636
https://doi.org/10.17576/jkukm-2020-32(4)-10

Effect of Intercritical Annealing on the Microstructural and Mechanical Behaviours of Dual-Phase Steels

Nora Osman, Zainuddin Sajuri[a*], Intan Fadhlina Mohamed[a], Mohd Zaidi Omar[a] & Syarif Junaidi[b]

[a]*Faculty of Engineering & Built Environment, Universiti Kebangsaan Malaysia, Malaysia*
[b]*Department of Mechanical and Nuclear Engineering, College of Engineering, University of Sharjah, Sharjah 27272, UAE*

**Corresponding author: zsajuri@ukm.edu.my*

Received 03 March 2020, Received in revised form 09 June 2020
Accepted 01 July 2020, Available online 30 November 2020

ABSTRACT

The automotive industry is the main consumer of dual-phase (DP) steels which have relatively impressive mechanical strength. DP steels are also known to have good ductility and load-bearing property because of their hard martensitic microstructure in soft ferrite grains. The main objective of this study is to determine the mechanical behaviour of DP steels with various martensite volume fractions. A heat treatment with an intermediate quenching procedure followed by three different intercritical temperatures is conducted to produce various ferrite–martensite containing DP steels with different martensite volume fractions (V_m). V_m affects the mechanical properties of steel, such as work hardening, ultimate tensile strength, yield strength and hardness. The results of the experiments conducted in this study prove that excellent work hardening and ductility are observed for DP steels with a low amount of martensite phase. Meanwhile, DP steels with high V_m exhibit high tensile strength and hardness with low ductility. Considère criterion is used to analyse the work hardening behaviour of DP steels. Results indicate that a one-stage work hardening takes place in DP steels; according to Considère criterion, instability strain or uniform elongation is also slightly increased by decreasing the martensite volume fraction or increasing the work hardening rate.

Keywords: Dual-phase steel; instability strain; intercritical annealing; intermediate quenching; martensite volume fraction.

INTRODUCTION

Dual-phase (DP) steels, also known as structural steels, are unique because they exist in two phases, namely, martensitic and ferritic phases. DP steels are primarily and widely used in chemical and civil engineering (e.g. building structures, bridges, ships and heavy vehicles) (Yousef Mazaheri et al. 2014; Og 2009)e.g. 540MPa. DP steels have several advantages, such as continuous yielding, high ultimate tensile strength (UTS), highly uniform and total elongation (TE), high initial strain-hardening rate and low elastic limit (Calcagnotto et al. 2011). The main alloying elements of DP steels are dominated by carbon, manganese and silicon. DP steels can also be heat-treated to produce hard structures with high yield strength which is a key advantage (Wei et al. 2013).

DP steels have a unique combination of two phases: hard martensite provides alloy strength, whereas soft ferrite offers formability. Ferrite obtains its strength from initial dislocation density. The rapid cooling that causes austenite to transform into martensite also results in compatibility stresses and strains which lend ferrite additional strength. However, the martensitic phase only relies on carbon content for strength (Ramazani et al. 2012). The main characteristics of DP steels are low initial flow stress, continuous yielding behaviour and a high initial work-hardening rate (Das & Chattopadhyay 2009). The as-received structure of DP steels—before heat treatment is applied to produce DP steels—is a low carbon steel, which comprises a mixture of deformed ferrite and pearlite phases. The heat treatment process for the enhancement of DP steels is known as intercritical annealing, where DP steels are heat-treated at a predetermined intercritical temperature to assist the recrystallisation of ferrite and to acquire different morphologies and V_m for DP steels (Ramazani et al. 2012; Syarif et al. 2018; Zheng & Raabe 2013. The recrystallisation process of ferrite evolves to a significant degree before pearlite (P) and ferrite (**α**) start to transform into austenite (**γ**). This depends on the strain energy stored in ferrite grains and the heating rate (Ghaheri & Honarmand 2014; Zheng & Raabe 2013).

During the first heat treatment known as the solution heat treatment or austenisation with isothermal holding time, a two-phase microstructure that comprises ferrite and austenite is obtained upon quenching in water. Subsequently, intercritical annealing takes places, and subsequent quenching causes the remaining austenite to transform into martensite, resulting in DP steels acquiring

ferrite and martensite morphology. However, Das & Chattopadhyay (2009) reported that steel that has been subjected to intermediate quenching (IQ), which involves austenitising heat treatment followed by intercritical annealing, yields the best strength and ductility because of its superior work-hardening behaviour to the sample that underwent intercritical annealing only or the sample that underwent step quenching only (Bag et al. 1999). So far, strength and ductility have shown an important link with V_m (Das & Chattopadhyay 2009; Gündüz 2009; Movahed et al. 2009). Other studies have investigated the effect of alloying elements on DP steels (Matsuda et al. 2011; Nakada et al. 2009; Nouri et al. 2010), the relationship between continuous yielding behaviour and mobile dislocation in a ferrite matrix (Armstrong & Li 2015)and the link between mechanical properties and martensite morphology (Bag et al. 1999; Han et al. 2014; Ramazani et al. 2012). However, only few studies have investigated the link between DP steel work-hardening behaviour and V_m.

Considère criterion is the most well-known criterion to historically relate plastic instability with work hardening via a stress–strain curve, specifically, the deformation mechanics near the maximum point of the curve (Yasnikov et al. 2014). Considère criterion states that at a given plastic strain rate at the start of necking, work-hardening coefficient h drops below flow stress (σ) value, where $h = \frac{\partial \sigma}{\partial \varepsilon}_{\dot{\varepsilon}}$ = work hardening. The intercept of the curve of work hardening rate versus the curve of true strain ε and the curve of true stress σ versus true strain ε denotes instability strain, also known as necking strain (ε_n) or uniform strain. Therefore, the onset of necking that corresponds to Considère criterion is signalled by instability strain (ε_n). Previous literature has connected the empirical laws of the stress–strain relationship with the work hardening of metals (Armstrong & Li 2015; Hartt 1966; Jonas et al. 1976; Kocks & Mecking 2003). However, the work-hardening behaviour and instability strain (ε_n) of DP steels have not been extensively investigated.

Therefore, this study is conducted to determine the appropriate heat treatment process that involves the austenitising and intercritical annealing of a low carbon steel at different temperatures to produce 20%, 50% and 80% V_m DP steels and to identify the mechanical and microstructural properties of DP steels at these V_m. Furthermore, V_m has been linked with DP steel work-hardening behaviour. Therefore, various V_m can result in the best combination of strength and ductility for DP steels.

METHODOLOGY

In this study, S15C low carbon steel with carbon content of 0.157% was used for all investigations. Table 1 lists the chemical composition of the steel used. Manganese and silicon are the main alloying elements other than carbon. Note that 20%, 50% and 80% V_m DP steels were the targets of this study. The amount of martensite forms in DP steels mainly depends on the volume percentage of austenite form of iron at which determined by the temperature at the time when quenching is performed.

To identify the suitable intercritical annealing temperatures that correspond to the aimed V_m, JMatPro® ver. 4.0, Sente software Ltd., Surrey, UK was used to model the phase equilibrium diagram of the steel at a temperature range of 700 ˚C–900 ˚C. The result of the JMatPro® is shown in Figure 1, where α-ferrite and γ-austenite were found to exist in the steel. From the result, the intercritical annealing temperatures that correspond to the 20%, 50% and 80% V_m were identified as 702 ˚C, 802 ˚C and 837 ˚C, respectively. A diagram for the heat treatment procedure was developed on the basis of the result of the JMatPro® analysis. The heat-treatment schedules, namely, the solution treatment at 1000 ˚C and the intercritical annealing at three different temperatures, that is, 732 ˚C, 802 ˚C and 837 ˚C were applied on steel bar specimens to obtain DP steel samples with 20%, 50% and 80% V_m; the samples were named as M20, M50 and M80, respectively. The holding time during the heat treatment process was 60 minutes. Details of the processes are indicated in Figure 2. A 2% nital (95% ethanol and 5% nitric acid) solution was used to etch the microstructures of the heat-treated samples. Subsequently, optical microscopy was used to further study the samples. ImageJ software was used to analyse the ferrite and martensite volume fractions in the steel by acquiring at least five digital optical micrographs for each sample set. Vickers hardness (HV) was measured at a 10 kgf load by a Shimadzu HMV-2000 hardness machine. A total of 10 indentation points were taken to obtain the average hardness of each sample.

The machining of S15C round bar into dumbbell tensile specimen shape was performed before conducting the heat treatment procedure. The specimen dimension was prepared according to ASTM standards: E8M-96. The gauge dimension of the specimen was Ø3 mm x 30 mm. A computer-controlled Z100 Zwick-Roell universal testing machine (maximum capacity of 100 kN) was used to conduct the tensile test. The accurate measurement of the strain throughout the test was performed using an extensometer. The tensile test was conducted at a crosshead speed of 0.15 mm/min in room temperature. The load versus elongation data were recorded to determine the standard tensile properties of the specimens. Each parameter of the three tensile specimens was tested, and the average values were reported. The work-hardening rate of the steel samples was analysed using the recorded tensile datasets and Considère criterion.

RESULTS AND DISCUSSION

DP STEEL MICROSTRUCTURE

Figure 3 illustrates the optical micrographs of the as-received S15C low carbon steel and the micrographs of the steel subjected to heat treatment to produce ferrite–martensite DP microstructures. Figure 3(a) shows a ferrite-pearlite phase of the as-received low carbon steel. The

bright phase is ferrite, whereas the dark phase is pearlite. The heat-treated specimens produced fine and uniform martensite (dark grains) distributed in the ferrite matrix (bright phase), as shown in Figures 3(b)–2(d) for the samples of M20, M50 and M80 that were heat-treated at intercritical temperatures of 702 ˚C, 802 ˚C and 837 ˚C, respectively. The DP steel specimen had a martensitic structure after water quenching from the solution heat treatment process. The martensite decomposes to ferrite and austenite phases upon reheating in the intercritical (α+γ) region and becomes ferrite+martensite DP structure via water quenching from the region. This martensitic transformation involves the sudden reorientation of C and Fe atoms from the γ-Fe (austenite) with FCC solid solution to a martensitic body-centred tetragonal solid solution (Mohanty et al. 2011; Syarif et al. 2018).

The effect of intercritical annealing temperature on Vm obeys the DP ferrite–austenite lever rule, as illustrated in Figure 1. It indicates that a temperature increase resulted in increased Vm (Li et al. 2013; Mazaheri et al. 2014). The raise of the intercritical temperature during the heat treatment significantly increases the martensite volume fraction. This situation conforms the DP ferrite–austenite lever rule. The lever rule states that the austenite volume fraction is accumulated as the temperature increases; subsequently, quenching in the water can transform it into martensite (Kulakov et al. 2014). Therefore, Vm increases at a high rate as the intercritical temperature increases. Furthermore, approximately equiaxed martensitic morphology was observed in the M20 and M50 samples, whereas the M80 sample showed needle-like and coarse martensitic morphology.

MECHANICAL ANALYSIS

The as-received S15C low carbon steel had a hardness value of 123 HV. The hardness of the heat-treated samples with increasing intercritical heat treatment temperatures is shown in Figure 4. The heat-treated samples had higher hardness than the as-received samples where the M80 sample exhibited 2.3 times higher hardness (270–311 HV) than the as-received sample (120–127 HV). The reason is that DP steels have martensite, which is hard and brittle and contributes to its high hardness.

The stress–strain curves of DP steels are illustrated in Figure 5. DP steels exhibit continuous yielding behaviour. This phenomenon is attributed to plastic deformation that occurs in the ferrite when austenite transforms into martensite, which results in unpinned dislocations (Balliger & Gladman 2014; Kumar et al. 2008). Kumar et al. (2008) and Movahed et al. (2009) claimed that at the early stage of plastic deformation, these unpinned dislocations are mobile and primarily located at the boundaries of the ferrite–martensite. Han et al. (2014) also pointed out that discontinuous yielding and large yield point elongation are caused by the easily deformed soft equiaxed-shape ferrite grains with low dislocation density at the early stage of the tensile test.

The stress–strain curves in Figure 5 also exhibit that DP steels had better tensile strength than the as-received sample because the pearlite in the as-received sample was replaced by a hard martensite phase after the IQ process. In DP steels, martensite performs as a reinforcement structure (Ramazani et al. 2012). Furthermore, DP steels by the IQ procedure had a better tensile property than the as receive

TABLE 1. Chemical composition of low carbon steel (wt%)

C	Si	Mn	P	S	Ni	Cr	Fe
0.157	0.22	0.458	0.0167	0.0176	0.0757	0.0303	Bal.

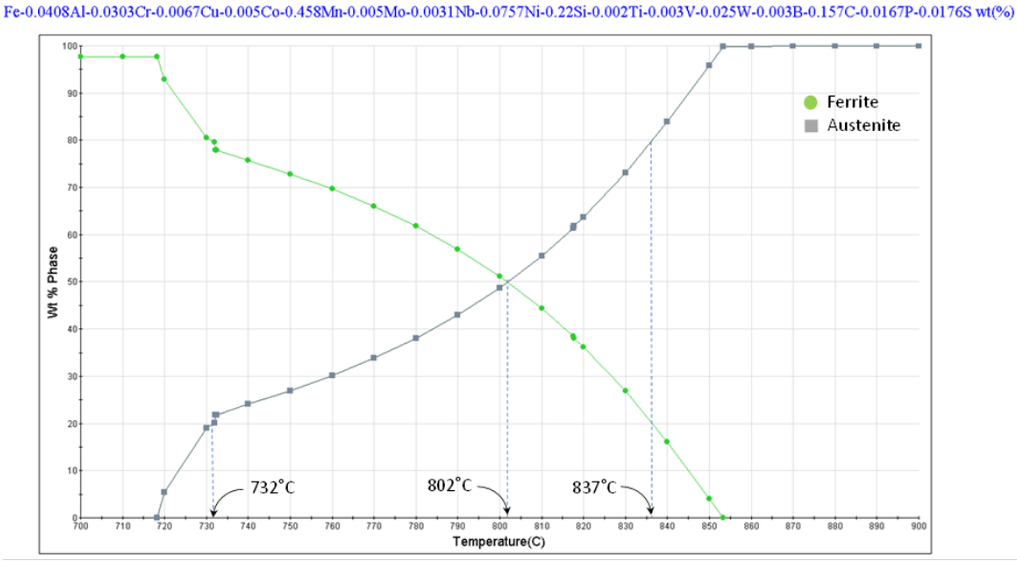

FIGURE 1. Phase equilibrium diagram of S15C low carbon steel obtained from JMatPro® simulation software.

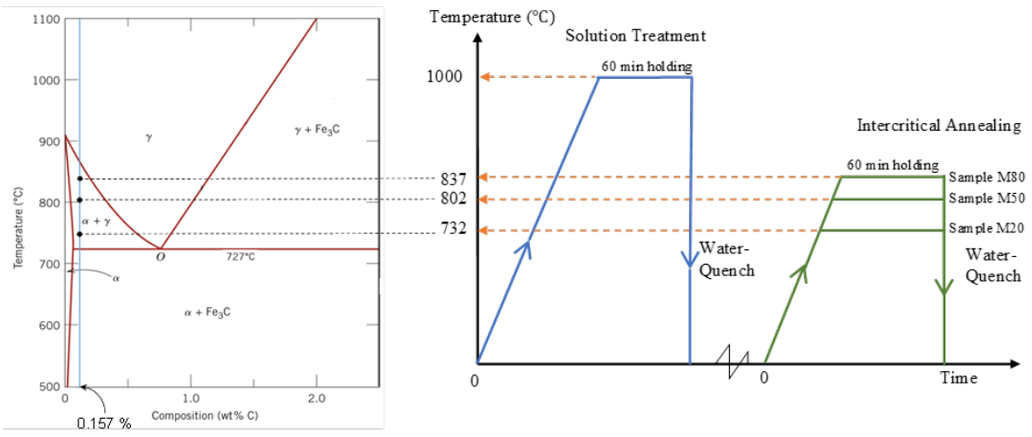

FIGURE 2. A shematic for the solution treatment and intercritical annealing at different temperatures, and the phase diagram of Fe-Fe_3C.

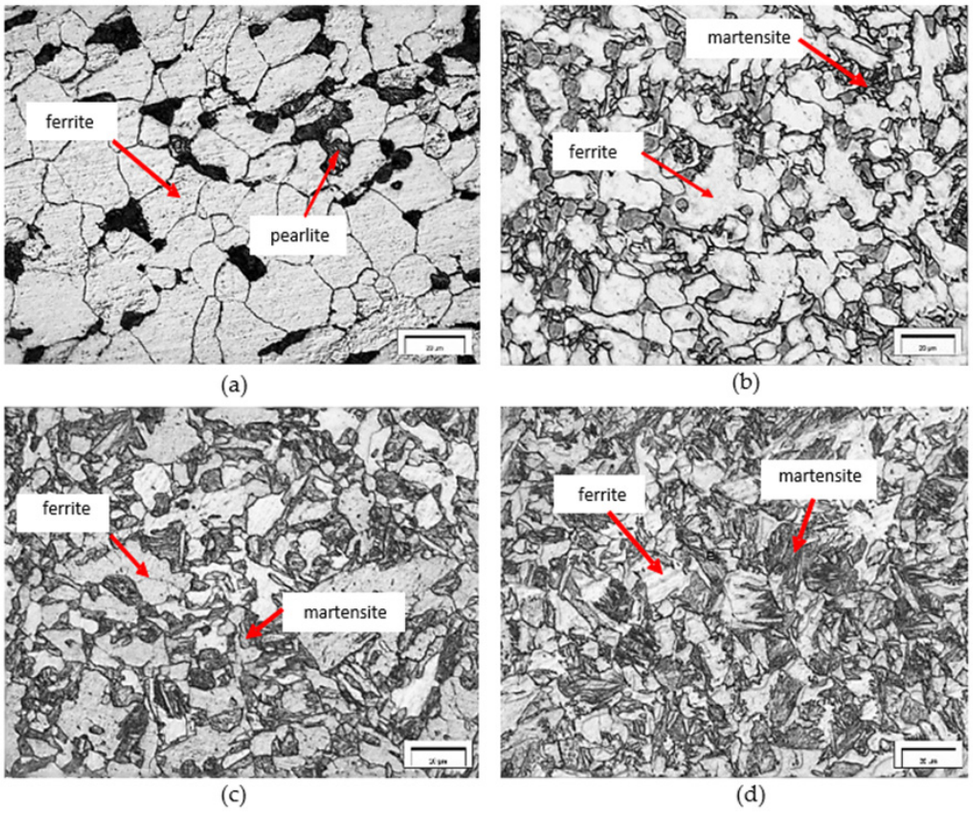

FIGURE 3. Optical micrographs of : (a) as-received low carbon steel with pearlite (dark) and ferrite (bright) phases, and (b)-(d) DP steels showing microstructure with martensite (dark) and ferrite (bright) phases for M20, M50 and M80 samples with 20, 50 and 80% martensite volume fraction

sample because the IQ specimens had an even distribution of martensite ensuing in a uniform distribution of dislocations (Ghaheri & Honarmand 2014). However, for the M80 sample with a greater amount of martensite than the M20 and M50 samples, high expansion occurred during austenite to martensite transformation (Park et al. 2014).

Therefore, the dislocation with high concentration around the brittle martensite phase causes the ferrite phase under pressure. This high concentration accumulates additional locked dislocations, resulting in high tensile values (Lee & Tyne 2011; Park et al. 2014). However, as the martensite becomes coarse, the ferrite matrix reduces and results in initial plasticity reduction. This phenomenon promotes increment in local internal stresses within the ferrite/martensite interface during plastic deformation (Mazaheri et al. 2015; Nouroozi et al. 2018; Park et al. 2014). As the martensite is connected and continuous, vacancies grow with less plastic strain and cause significant

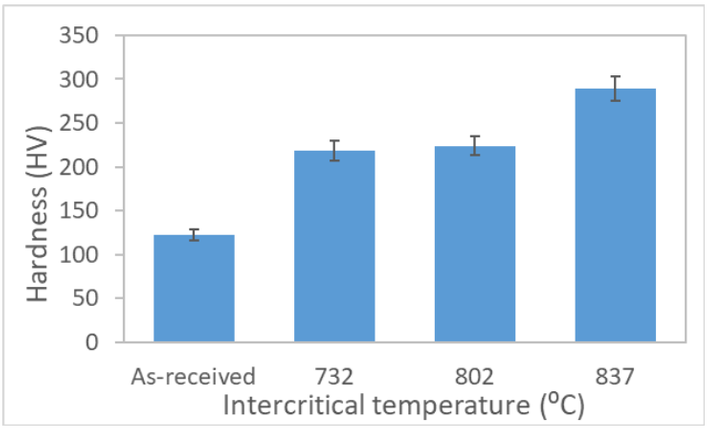

FIGURE 4. Hardness variation as a function of intercritical temperature.

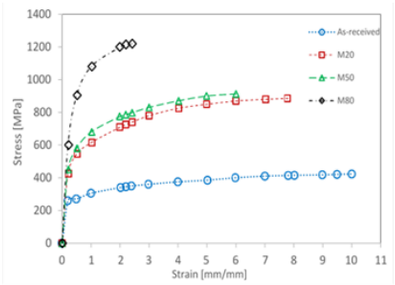

FIGURE 5. Stress vs strain curve of the as-received and the DP steels

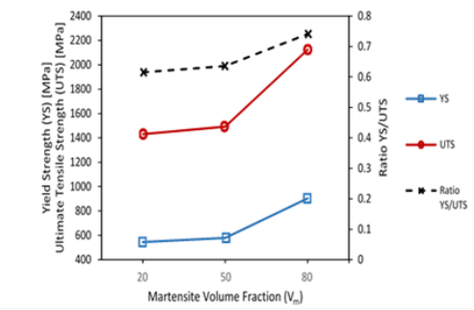

FIGURE 6. Yield stress (YS) , ultimate tensile strength (UTS) and ratio YS/UTS as a function of martensite volume fraction (V_m)

decrease in ductility (Nouroozi et al. 2018; Pouranvari 2010). This situation explains the brittle fracture in the M80 sample, which had less elongation than other samples, and relies on the martensite fracture manner in the ferrite matrix and martensite fracture during necking.

Figure 6 shows the ratio of yield strength to the ultimate strength of the heat-treated samples as a function of V_m and the variation of ultimate strength and yield stress. The work hardenability of DP steels, that is, the ability of DP steels to withstand the maximum load of plastic deformation is indicated by the ratio of yield strength to ultimate strength; the higher the ratio, the higher the rate at which the steels can be hardened and the smaller the ratio, the more the steels can further stretch and the more resistant these steels are to plastic deformation (Balbi et al. 2018). The M20 sample showed the lowest ratio amongst all samples. Processes that involve plastic deformation, such as the making of car body structures, favour materials with low ratio values.

UTS was multiplied with TE to determine DP steel workability. The effect of V_m on DP steel workability is shown in Figure 7. The UTS × TE value is an indicator of DP steel workability. The sample with high UTS × TE value exhibited great workability, where the M20 sample had higher workability than the M50 and M80 samples. The combination of UTS and ductility indicates the effective workability, which is an important property for automotive and structural industries, of the sample.

Figure 8 illustrates Considère criterion, that is, the curve of work hardening rate ($\delta\sigma/\delta\varepsilon$) versus true strain ($\varepsilon$) and the curve of true stress (σ) versus true strain (ε). From the true stress–true strain curves of the M20, M50 and M80 samples, a monotonic decrease was observed in the strain at the uniform deformation area. All samples showed identical curve patterns; before the intercept, an initial decline was observed, but after the intercept, the work hardening rate shot up immediately. From Figure 8, despite the initial drop, the work hardening rate was still maintained above the true stress value up until plastic instability. Therefore, deformation occurred near the plastic instability point where necking was initiated, that is, at the point where the curve of $\delta\sigma/\delta\varepsilon$ versus ε intersected with the curve of σ versus ε, at which point the work hardening rate also dropped rapidly. This observation is in agreement with the engineering concept of UTS (Byun et al. 2004; Ramazani et al. 2012). Figure 8 also illustrates that uniform strain or instability strain is proportional to work hardening rate; the sample with high instability strain had a high work hardening rate. The larger the instability strain, the higher the deformation rate of the steel before it reaches the instability state; in which the steel can plasticise at a high rate before necking occurs (Byun et al. 2004; Yasnikov et al. 2014).

From Figure 8, the M20 sample showed the highest instability strain with a value of 0.06. Ramazani et al. (Ramazani et al. 2012) used Considère criterion to connect

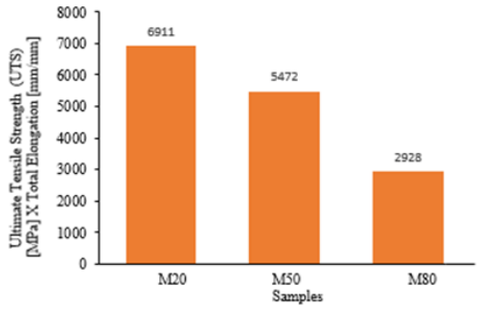

FIGURE 7. Ultimate strength [UTS] x total elongation [TE] as a function of different martensite volume fractions

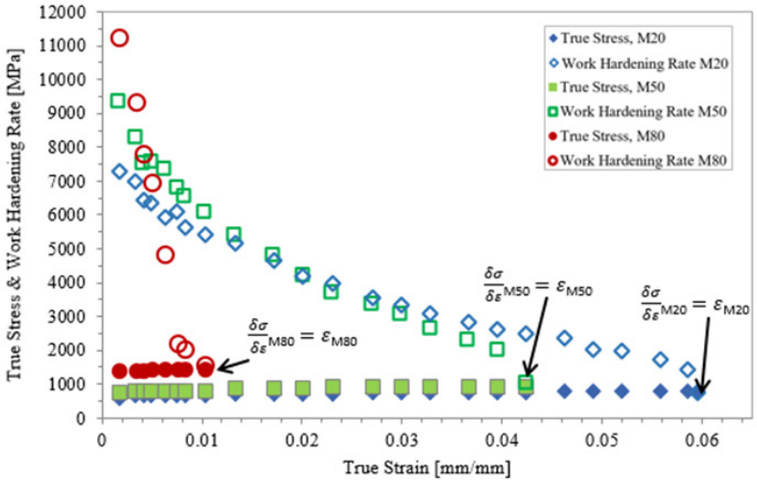

FIGURE 8. The effect of martensite volume fraction (V_m) on the work hardening behaviour of DP steel containing 20, 50 and 80% volume fraction of martensite

instability strain with V_m, where a decrease in V_m was observed to cause a slight increase in instability strain. Furthermore, Bag et al. (Bag et al. 1999) conducted a fractographic analysis of the tensile deformation of DP steels. They found that the first to deform was ferrite, and this deformation caused the accelerated nucleation of cracks at the ferrite/martensite interfaces or when precipitation occurred. Subsequently, these cracks propagated via cleavage fracture or dimple mode. Precipitates predominantly cause the crack initiation site in DP with $V_m < 45\%$. If the V_m is approximately 50%, then the crack initiation site predominantly occurs at the ferrite/martensite interfaces due to the absence of precipitates.

Meanwhile, several fine dimples were produced due to the huge crack initiation site occurring in DP steels with very high V_m. Thus, the sample with high V_m and a coarse structure may have reduced microstructural inhomogeneity because the ferrite–martensite microstructure of the sample experiences average internal stress, which slightly affects the microstructure at the beginning of the post-instability strain (Balbi et al. 2018). The above findings agree with the current microstructural analysis presented in Figures 2 and 3, which show that the M20 sample had the lowest V_m and a high instability strain due to few crack initiation sites that can reduce its strength.

Therefore, the M20 sample exhibited the most desirable properties for DP steels and showed a good combination of the lowest yield to UTS ratio, the highest magnitude of instability strain and good strength and ductility.

CONCLUSION

In this study, an intermediate quench heat treatment was used to produce various ferrite-and-martensite-containing DP steels with different martensite volume fractions. The intercritical heat treatment temperature resulted in increased V_m. Excellent mechanical properties, such as workability, ductility and tensile strength, were observed for DP steels containing low martensite phases (approximately less than 50% V_m). Tensile strength, yield strength and elongation decreased as V_m increased, but the hardness increased. This result is in accordance with Considère criterion, which states that instability strain slightly increases as V_m decreases.

ACKNOWLEDGEMENT

The authors would like to thank Universiti Kebangsaan Malaysia for their financial support under the research grant FRGS/1/2013/TK01/UKM/02/4.

DECLARATION OF COMPETING INTEREST

None.

REFERENCES

Armstrong, R. W. & Li, Q. 2015. Dislocation mechanics of high-rate deformations. *Metallurgical and Materials Transactions A: Physical Metallurgy and Materials Science* 46(10): 4438–4453.

Bag, A., Ray, K. K. & Dwarakadasa, E. S. 1999. Influence of martensite content and morphology on tensile and impact properties of high-martensite dual-phase steels. *Metallurgical and Materials Transactions A: Physical Metallurgy and Materials Science* 30(5): 1193–1202.

Balbi, M., Alvarez-Armas, I. & Armas, A. 2018. Effect of holding time at an intercritical temperature on the microstructure and tensile properties of a ferrite-martensite dual phase steel. *Materials Science and Engineering A* 733: 1–8.

Balliger, N. K. & Gladman, T. 2014. Work hardening of dual-phase steels. *Metal Science* 15(3): 95–108.

Byun, T. S., Hashimoto, N. & Farrell, K. 2004. Temperature dependence of strain hardening and plastic instability behaviors in austenitic stainless steels. *Acta Materialia* 52(13): 3889–3899.

Calcagnotto, M., Adachi, Y., Ponge, D. & Raabe, D. 2011. Deformation and fracture mechanisms in fine- and ultrafine-grained ferrite/martensite dual-phase steels and the effect of aging. *Acta Materialia* 59(2): 658–670.

Das, D. & Chattopadhyay, P. P. 2009. Influence of martensite morphology on the work-hardening behavior of high strength ferrite-martensite dual-phase steel. *Journal of Materials Science* 44(11): 2957–2965.

Ghaheri, A., Shafyei, A. and Honarmand, M., 2014. Effects of inter-critical temperatures on martensite morphology, volume fraction and mechanical properties of dual-phase steels obtained from direct and continuous annealing cycles. *Materials & Design (1980-2015)* 62: 305-319.

Gündüz, S. 2009. Effect of chemical composition, martensite volume fraction and tempering on tensile behaviour of dual phase steels. *Materials Letters* 63(27): 2381–2383.

Han, J., Lee, S., Jung, J. & Lee, Y. 2014. The effects of the initial martensite microstructure on the microstructure and tensile properties of intercritically annealed Fe – 9Mn – 0. 05C steel. *Acta Materialia* 78: 369–377.

Hartt, E. W. 1966. Theory of the Tensile Test. *Acta Metallurgica* 15: 351–355.

Jonas, J. J., Holt, R. A. & Coleman, C. E. 1976. Plastic stability in tension and compression. *Acta Metallurgica* 24(10): 911–918.

Kocks, U. F. & Mecking, H. 2003. Physics and phenomenology of strain: the FCC case. *Progress in Materials Science* 48: 171–273.

Kulakov, M., Poole, W. J. & Militzer, M. 2014. A microstructure evolution model for intercritical annealing of a low-carbon dual-phase steel. *ISIJ International* 54(11): 2627–2636.

Kumar, A., Singh, S. B. & Ray, K. K. 2008. Influence of bainite/martensite-content on the tensile properties of low carbon dual-phase steels. *Materials Science and Engineering A* 474(1–2): 270–282.

Lee, S. & Tyne, C. J. V. A. N. 2011. A kinetics model for martensite transformation in plain carbon and low-alloyed steels. *Metallurgical and Materials Transactions A* 43(2): 422-427.

Li, P., Li, J., Meng, Q., Hu, W. & Xu, D. 2013. Effect of heating rate on ferrite recrystallization and austenite formation of cold-roll dual phase steel. *Journal of Alloys and Compounds* 578: 320–327.

Matsuda, H., Seto, K., Hasegawa, K., Toji, Y., Nakajima, K., Yamashita, T. & Okuda, K. 2011. Effect of Mn partitioning during intercritical annealing on following γ→α transformation and resultant mechanical properties of cold-rolled dual phase steels. *ISIJ International* 51(5): 818–825.

Mazaheri, Y, Kermanpur, A. & Najafizadeh, A. 2015. Microstructures, mechanical properties , and strain hardening behavior of an ultrahigh strength dual phase steel developed by intercritical annealing of cold-rolled ferrite / martensite. *Metallurgical and Materials Transactions A* 46(7): 3052-3062.

Mazaheri, Yousef, Kermanpur, A. & Najafizadeh, A. 2014. A novel route for development of ultrahigh strength dual phase steels. *Materials Science and Engineering A* 619: 1–11.

Mohanty, R. R., Girina, O. A. & Fonstein, N. M. 2011. Effect of heating rate on the austenite formation in low-carbon high-strength steels annealed in the intercritical region. *Metallurgical and Materials Transactions A: Physical Metallurgy and Materials Science* 42(12): 3680–3690.

Movahed, P., Kolahgar, S., Marashi, S. P. H., Pouranvari, M. & Parvin, N. 2009. The effect of intercritical heat treatment temperature on the tensile properties and work hardening behavior of ferrite-martensite dual phase steel sheets. *Materials Science and Engineering A* 518(1–2): 1–6.

Nakada, N., Takaki, S., Murakami, M., Tsuchiyama, T. & Imanami, Y. 2009. Contribution of soft copper particle on work hardening behavior in ferritic iron. *ISIJ International* 49(8): 1225–1228.

Nouri, A., Saghafian, H. & Kheirandish, S. 2010. Effects of silicon content and intercritical annealing on manganese partitioning in dual phase steels. *Journal of Iron and Steel Research International* 17(5): 44–50.

Nouroozi, M., Mirzadeh, H. & Zamani, M. 2018. Effect of microstructural refinement and intercritical annealing time on mechanical properties of high-formability dual phase steel. *Materials Science & Engineering A*. 736 (2018): 22-26.

Og, K. 2009. Effect of various dual-phase heat treatments on the corrosion behavior of reinforcing steel used in the reinforced concrete structures 23: 78–84.

Park, K., Nishiyama, M., Nakada, N. & Tsuchiyama, T. 2014. Materials science & engineering a effect of the martensite distribution on the strain hardening and ductile fracture behaviors in dual-phase steel. *Materials Science & Engineering A* 604: 135–141.

Pouranvari, M. 2010. Tensile strength and ductility of ferrite-martensite dual phase steels. *Association of Metallurgical Engineers of Serbia AMES* 16(3): 187–194.

Ramazani, A., Mukherjee, K., Prahl, U. & Bleck, W. 2012. Modelling the effect of microstructural banding on the flow curve behaviour of dual-phase (DP) steels. *Computational Materials Science* 52(1): 46–54.

Syarif, J., Handra, N., Sajuri, Z. & Omar, M. Z. 2018. Change in tensile properties of dual-phase steels by Cu addition 71(2): 513–519.

Wei, R., Enomoto, M., Hadian, R., Zurob, H. S. & Purdy, G. R. 2013. Growth of austenite from as-quenched martensite during. *Acta Materialia* 61(2): 697–707.

Yasnikov, I. S., Vinogradov, A. & Estrin, Y. 2014. Revisiting the Considère criterion from the viewpoint of dislocation theory fundamentals. *Scripta Materialia* 76: 37–40.

Zheng, C. & Raabe, D. 2013. Interaction between recrystallization and phase transformation during intercritical annealing in a cold-rolled dual-phase steel: A cellular automaton model. *Acta Materialia* 61(14): 5504–5517.